Supplementary Information

Spring-programmable multi-feature hyperelastic mechanical metamaterials

Haoyuan Guo, and Jianxun Zhang*

Supplemental Text

Ⅰ. Conceptual interpretation

Briefing on spiral spring: A coil spring is a coil part. When subjected to force, it has a certain expansion and contraction space and can store and release energy. The basic properties of coil springs include three items. The elastic deformation capacity refers to the ability of a coil spring to undergo elastic deformation under the action of an external force and store energy. When the external force disappears, the spring can return to its original shape and simultaneously release the stored energy. Load-bearing refers to the fact that the coil spring can withstand certain loads, including compressive force, tensile force and torsional moment, etc. Its load-bearing capacity depends on parameters such as the material of the spring, wire diameter, number of turns, and pitch. Stability refers to the ability of a coil spring to maintain stable performance during operation. There are nine performance parameters of coil springs (Fig. S1G). The wire diameter d refers to the diameter of the spring wire, which determines the stiffness and load-bearing capacity. The inner diameter D_1 is the minimum diameter of the coil spring. The outer diameter D_2 is the maximum diameter of the coil spring. Pitch t is the variation distance of the head and tail ends of a coil spring wire on the axis. The elastic coefficient K_s is the reaction force generated per unit length when the spring is deformed by an external force in axial direction, and it is used to measure the stiffness of the spring. The effective number of turns n affects the load-bearing capacity of the spring. The number of supporting turns n_2 determines the stability of the spring. The free length L refers to the length value of the spring when no external force is applied to both ends. The working length L_0 refers to the actual deformable length of a spring from one end to the other when it is subjected to an external force. This length is the part of the spring that effectively stores and releases energy when it is compressed or stretched.

Briefing on syncretic-bionic corrugated orthogonal layering configuration: Organisms in nature have acquired the optimal structural composition that can adapt to their living environment during the long-term process of evolution, and have brought about mechanical properties that can meet the structural functions. The finned mantis shrimp preys by the high-speed impact of its claws. The instantaneous speed of the claws can reach 23 m s^{-1}, and they may withstand an acceleration of more than 100 km s^{-2} and an impact force of 1.5 kN. The ability to withstand such high-intensity impacts is attributed to the parallel layered fiber structure on the inner layer of the front toes of the shrimp claws, which are arranged in regular triangular corrugated units[1-4]. Meanwhile, research shows that the corrugated structure has excellent compressive resistance, bending resistance and energy absorption efficiency[5-7]. The fracture toughness of shells can reach 3,000 times that of ordinary pure calcium carbonate substances[8,9]. Shells can be classified into the cuticle, prismatic layer and nacre along the thickness direction. In the nacre, inorganic calcium carbonate or aragonite flakes are arranged in a layered form[10-12]. The layering angle refers to the angle between different layer directions and the matrix direction, which is a very important factor and can have a significant impact on multiple performance indicators such as strength, stiffness and fatigue life. Orthogonal layering can provide higher strength and rigidity. Therefore, we propose the concept of syncretic bionics, successively integrating the imitation of the parallel layered fiber structure of the pincers of the mantis shrimp, the structural reinforcement mechanism of the shell layered arrangement, and the concept of layering angles. We take the triangular corrugation as the basic unit and the multi-level orthogonal layering as the basic means (Fig. S2). To maximize the material property of TPU and enable it to undergo large elastic deformation, each surface of triangular corrugations has been hollowed out. Make them have square panes of uniform size one by one. In order to maintain its stability in the vertical direction during the deformation process and improve the energy dissipation capacity of the final configuration as much as possible, an X-shaped support is innovatively added to each square pane. The unit cell size is 100mm in length, 10mm in width and 10mm in height. 10 single cells are closely arranged and connected along the width direction, a square

corrugated single layer with a side length of 100mm is obtained. Then, multiple single layers are stacked along the height direction, with the angle between adjacent layers kept at 90°. A circle with a diameter of 100mm is used for tensile excision, and structures are designed at the bottom to be embedded and fixed with the spring-fixing circular plate according to the geometric relationship. Finally, the syncretic-bionic corrugated orthogonal layering configuration is obtained.

Hyperelasticity and modulus: Hyperelasticity is a concept in material mechanics, typically used to describe the highly nonlinear elastic behavior exhibited by certain materials (such as rubber, elastomers, and polymer materials, etc.) when subjected to large deformations. After being subjected to external forces, these materials can return to their original shapes and sizes, and during this process, the stress-strain relationship shows complex nonlinear characteristics. In elastic mechanics, "modulus" usually refers to the measurement of the relationship between stress and strain within the elastic deformation range of a material. For linear elastic materials, the modulus is a constant. For instance, the elastic modulus describes the proportional relationship between stress and positive strain when the material is stretched or compressed. However, in hyperelastic materials, due to the nonlinearity of the stress-strain relationship, the traditional concept of modulus is no longer applicable or needs to be redefined. Some approximate linear moduli or tangential moduli are introduced to describe the behavior of hyperelastic materials under specific deformation states.

Metamaterial densification: The state in which the corrugated orthogonal layering configuration is densified and the spring compression reaches the maximum is called metamaterial densification. Referring to the method of handling the compression curve of porous materials by Li et al.[13], when the corrugated orthogonal layering configuration reaches the maximum energy absorption efficiency, it is called densification. The definition of energy absorption efficiency is

$$\eta(\varepsilon)=\frac{1}{\sigma(\varepsilon)}\int_0^{\varepsilon}\sigma(\varepsilon)\mathrm{d}\varepsilon \qquad \backslash* \text{ MERGEFORMAT (1)}$$

The metamaterial densification can be divided into two situations. The first case is the rotation angle of the spring is θ=1080°, only the corrugated orthogonal layering configuration is compressed. The metamaterial densification is equivalent to that of the corrugated orthogonal layering configuration, and the densification displacement can be calculated according to Equation (1). The second situation is that the rotation angle of the spring is $0\le\theta<1080°$, The force after the corrugated orthogonal layering configuration is densified is not sufficient to compress the spring. Therefore, the orthogonal layering configuration will continue to be compressed until the compression force is sufficient to compress the spring, and during the spring compression process, the orthogonal layering configuration will be continuously compressed. Under this circumstance, the densification displacement is greater than the sum of the densification displacement of the orthogonal layering configuration and the maximum compression of the spring.

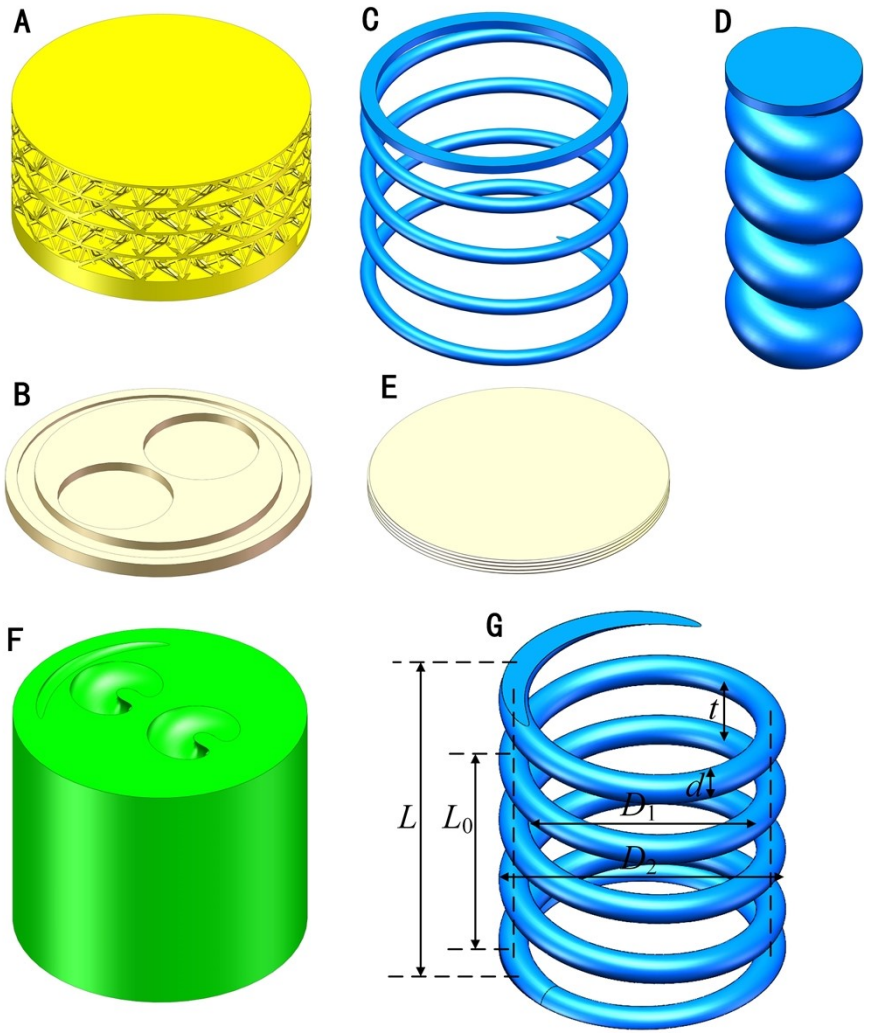

Fig. S1 Design of multi-feature spring-dominated hyperelastic dissipative metamaterial. (A) Syncretic-bionic corrugated orthogonal layering configuration. (B) Spring-fixing circular plate with grooves. (C) Outer spring. (D) Inner spring. (E) Spring adjusting plate with external threads. (F) Spring-fixing cylinder with internal threads. (G) Visualization of performance parameters of coil spring.

As shown in Fig. S1, the Spring-programmable multi-feature hyperelastic dissipative mechanical metamaterial is composed of a syncretic-bionic corrugated orthogonal layering configuration, a spring-fixing circular plate with grooves, two inner springs, an outer spring, and accessory components. In the metamaterial shown in Fig. 1a, the wire diameter d of the inner spring is 16mm, the inner diameter D_1 is 3mm, the outer diameter D_2 is 35mm, the pitch t is 20mm, the effective number of turns n is 3, the support number n_2 is 4, the free length L is 80mm, and the working length L_0 is 60mm. The wire diameter d of the outer spring is 5mm, the inner diameter D_1 is 76mm, the outer diameter D_2 is 86mm, the pitch t is 20mm, the effective number of turns n is 3, the support number n_2 is 4, the free length L is 80mm, and the working length L_0 is 60mm. First, insert the spring-fixing circular plate into the reserved gap on the syncretic-bionic corrugated orthogonal layering configuration. The spring-fixing circular plate can not only fix the inner and outer springs, but also ensure that the corrugated orthogonal layering configuration is uniformly compressed during the loading process. The inner-upper part of the spring-fixing cylinder has a cylinder with a height of 20mm. Inside, there is a hollow cut that is consistent with the contours of inner and outer springs. The spring is rotated into it and therefore fixed. Inner springs mainly play the role of bearing and energy dissipation, while the outer spring mainly serves to balance and stabilize the overall structure. The spring adjusting circular plate is connected to the spring-fixing cylinder through threads. The lower surfaces of springs are fixed after coincident with the upper surface of the spring adjusting circular plate, and the plate is not subjected to force during the loading process. By rotating the spring adjusting plate, the height position of itself in the spring-fixing column cylinder can be adjusted, thereby regulating the working length L_0 of springs and achieving the programmable effect of metamaterial (Video S1).

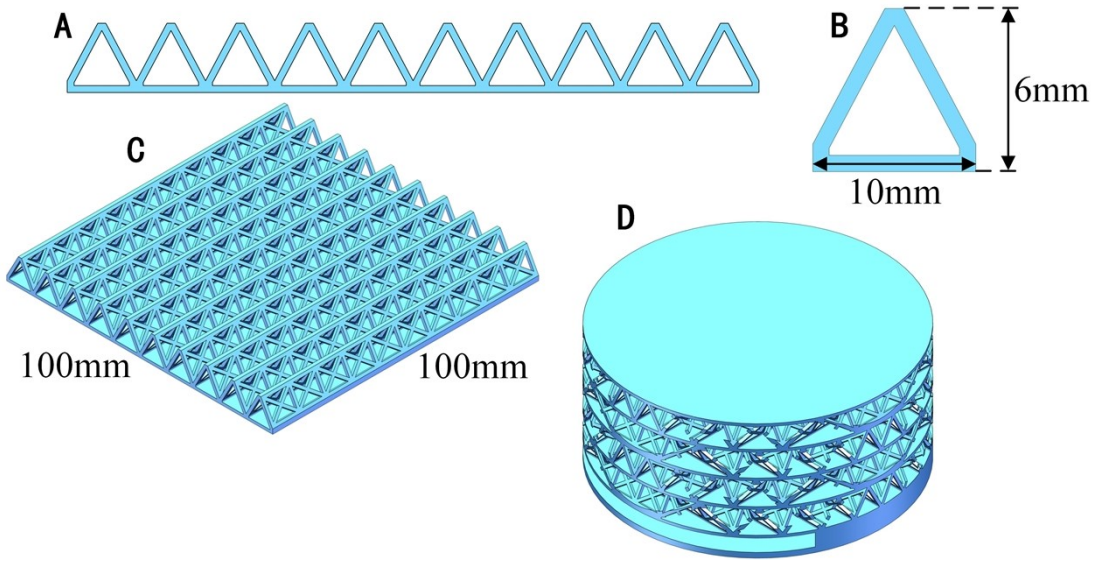

Fig. S2 Design of syncretic-bionic corrugated orthogonal layering configuration. (A) Side view of the corrugated layer. (B) Size of each corrugation. (C) Axonometric view of the corrugated layer. (D) Syncretic-bionic corrugated orthogonal layering configuration.

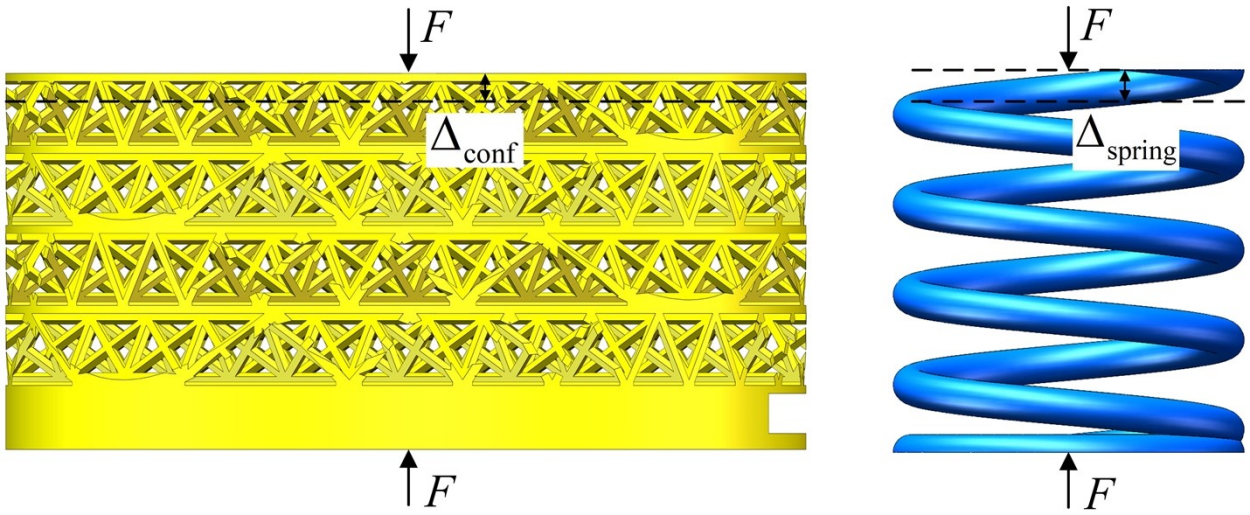

Fig. S3 Definitions of the instantaneous stiffness K_{ci} of the corrugated orthogonal layering configuration and the instantaneous stiffness K_{si} of the spring. When a pair of forces F of equal magnitude but opposite directions are applied to the upper and lower surfaces of the corrugated orthogonal layering configuration, the configuration will deform Δ-conf. at a certain moment. The instantaneous stiffness of the corrugated orthogonal layering configuration is $K_{ci} = F/\Delta_{conf}$. Similarly, when a pair of forces F of equal magnitude but opposite directions are applied to the upper and lower surfaces of the spring, the spring will deform Δ_{spring} at a certain moment. The instantaneous stiffness of the spring is $K_{si} = F/\Delta_{spring}$.

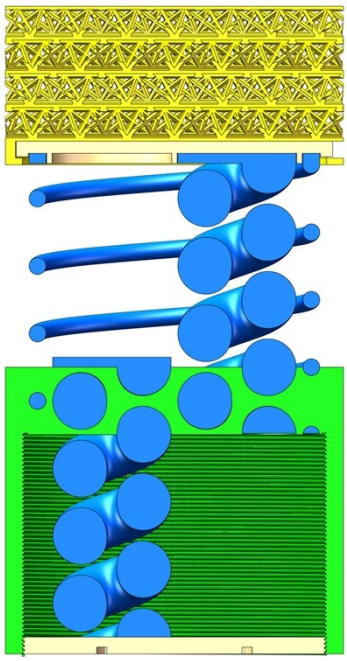

Fig. S4 The initial state where the total working length L_{0T} of springs is the same when metamaterial heights are different. When an inner spring has the maximum working length L_{01max}, its rotation angle is $\theta = 0°$ and clockwise rotation is positive. The rotation angle of the other inner spring is $\theta = 0°$ when it has the shortest working length L_{01min} and counterclockwise rotation is positive.

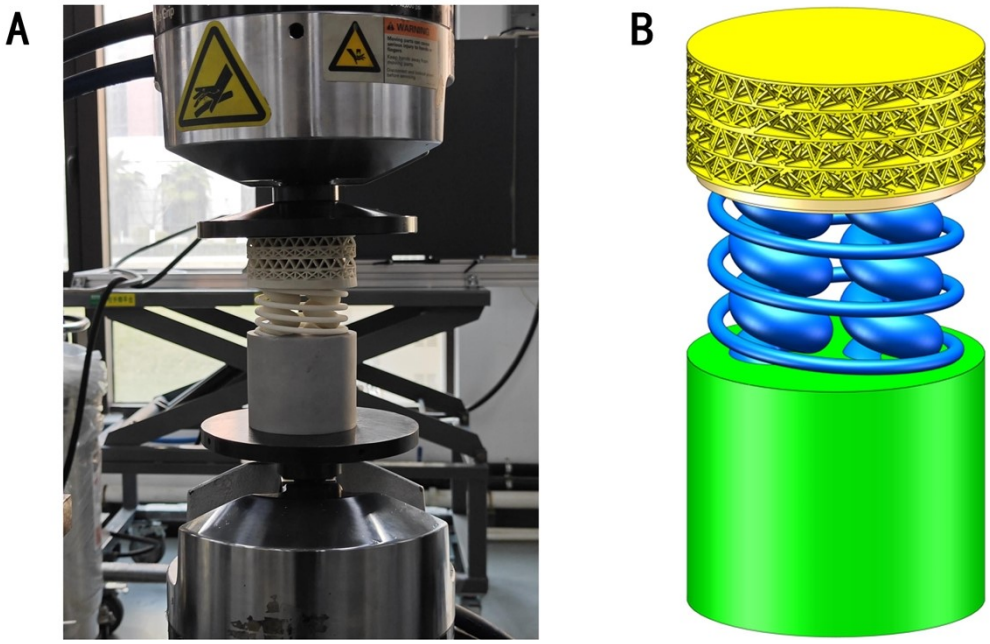

Fig. S5 Design of syncretic-bionic corrugated orthogonal layering configuration. (A) Experimental device. (B) Finite element model.

In order to improve the calculation efficiency, the experimental specimens are simplified to obtain the finite element model. The internal thread and the hollow cut consistent with the contour of inner and outer springs are removed foam the spring-fixing cylinder, and the cylinder is set as a rigid body. The solid springs are connected to the spring-fixing cylinder through

“Tie” constraints. Delete the spring adjustment circular plate with external threads. The grooves used to fix the inner and outer springs are removed from the spring-fixing circular plate. Inner springs only retain the working length corresponding to each rotation angle and the connection parts with the spring-fixing circular plate are deleted. The upper and lower ends of inner springs are respectively connected to the spring-fixing circular plate and the spring-fixing cylinder through “Tie” constraints. The outer spring is treated in the same way as inner springs. Delete the gap reserved on the syncretic-bionic corrugated orthogonal layering configuration for fixing the spring-fixed circular plate, and connect the two through “Tie” constraint.

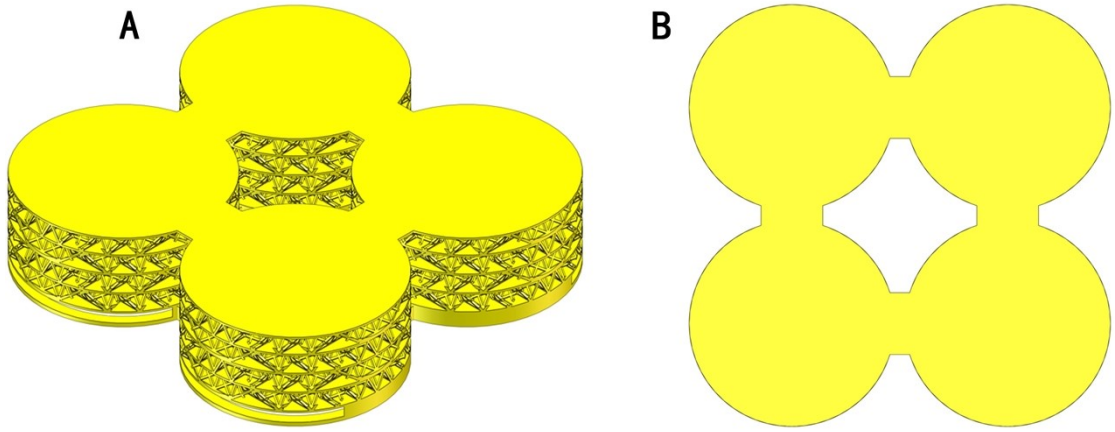

Fig. S6 Corrugated orthogonal layering configuration connection of the metamaterial group. (A) Axonometric views. (B) Top view.

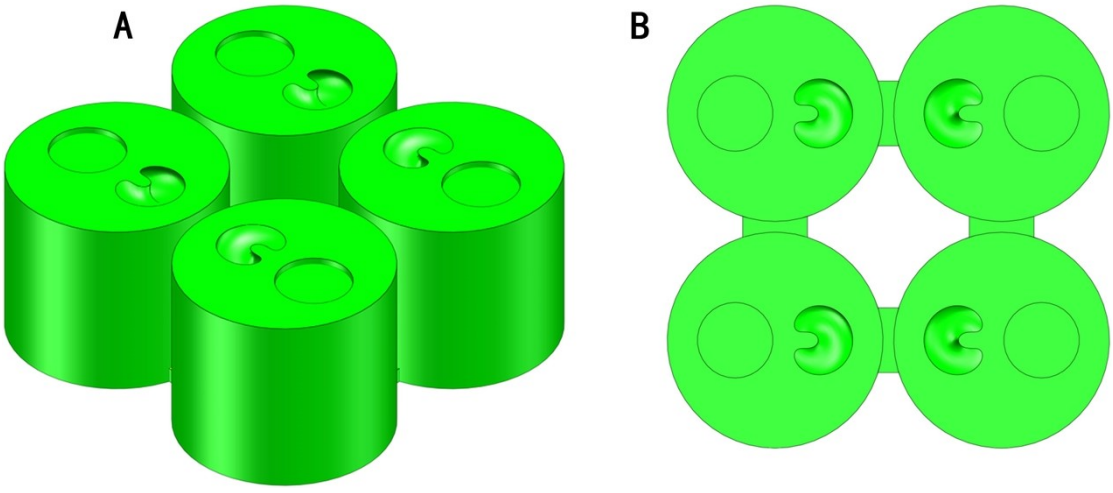

Fig. S7 Spring-fixing cylinder connection of the metamaterial group. (A) Axonometric views. In order to match higher springs, cylindrical grooves are designed on the spring-fixing cylinder. (B) Top view.

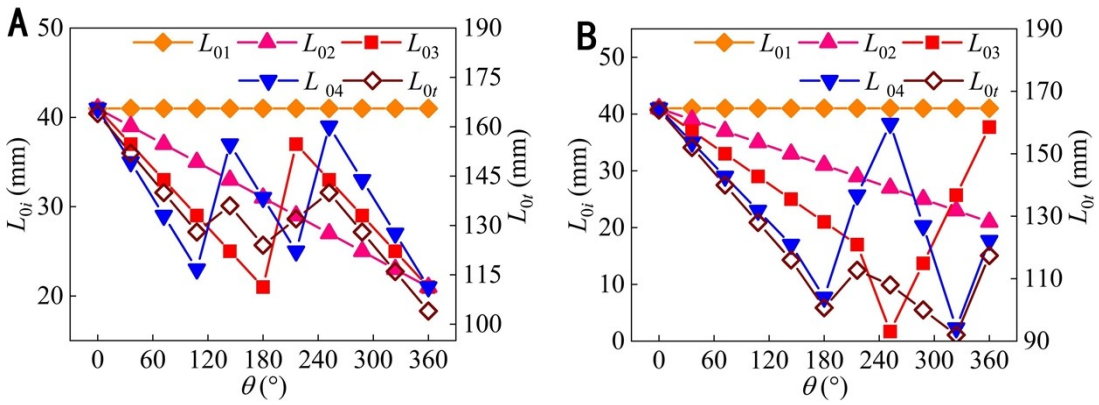

Fig. S8 Variation of the working length L_{0i} of springs in the variable rotation angle difference metamaterial group under difference adjustment rules as the rotation angle θ increases. (A) The variable rotation angle difference metamaterial group based on Rule 1. (B) The variable rotation angle difference metamaterial group based on Rule 2.

For the dimension of changing the adjustment rule of angles, the object we regulate is the variable rotation angle difference metamaterial group with the working length of lower springs $L_0 = 40mm$, and two adjustment rules are given respectively. Rule 1 is that when θ>360°, the part no greater than 360° of the extra angle is taken as the value of the rotation angle ,θ-$_i$.,=1,2,3,4.. Rule 2 is that when θ>500°, the extra angle is multiplied by 3 and then perform reverse cancellation. The two rules show different variation trends of the working length L_{0i} of each spring and the total working length L_{0t} of the springs inside metamaterial. The spring working length L_{0i} curves of the variable rotation angle difference metamaterial group based on Rule 1 and Rule 2 exhibits rich variability. In contrast, the total working length curve of lower springs based on Rule 1 shows four direction turns, and the same L_{0t} has at most five rotation angles corresponding to it. The L_{0t} curve of the metamaterial group based on Rule 2 presents a W shape. Looking at the working length L_{0i} curves of each lower spring separately, the change of the angle adjustment rule has no significant effect on L_{01} and L_{02}. For L_{03} and L_{04}, Rule 1 increases the frequency of their changes, while Rule 2 increases the amplitude of their changes.

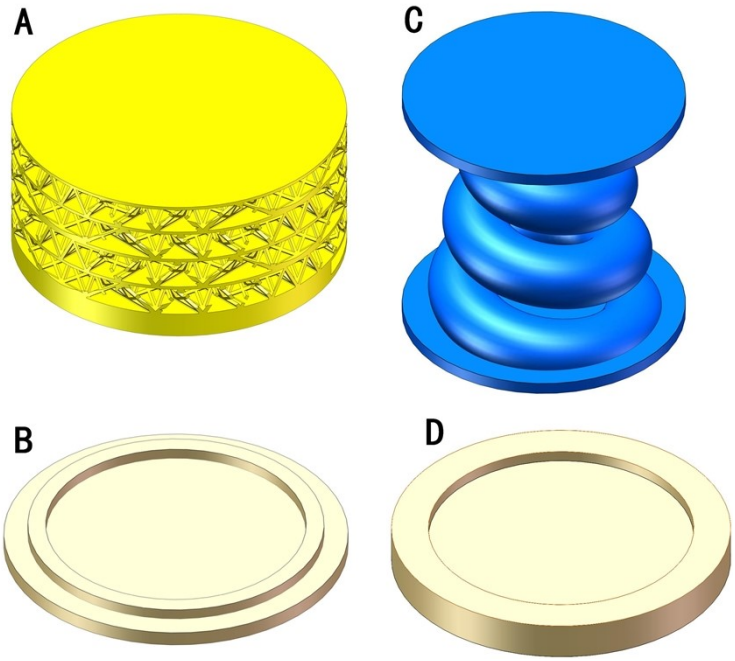

Fig. S9 Adjustable hyperelastic metamaterial design. (A) Syncretic-bionic corrugated orthogonal layering configuration. (B) Spring-fixing upper circular plate with a groove. (C) *D* non-uniform spring with law *D*1, the other two types of non-uniform springs are shown in Fig. 3 of the main text. (D) Spring-fixing lower cylinder with a groove.

As shown in Fig. S9, the tunable hyperelastic metamaterial is composed of a syncretic-bionic corrugated orthogonal layering configuration, non-uniform springs, and accessory components. In the metamaterials shown in Fig. 3a-c, there are two types of springs with non-uniform average diameters D=,,(D-$_1$.+,D-$_2$)../2. The wire diameter d is both 16mm and the pitch t is both 20mm. The average diameter D of the first type expands at an angle of 10° on the basis of 19mm, and the working length L_0 is 60mm. The second type of average diameter D expands by 30mm in opposite directions at angles of 10° and 25° respectively on the basis of 19mm, and the working length L_0 is 60mm. The wire diameter d of the spring with non-uniform pitch is 16mm, and the average diameter D is 19mm. The pitch increases by 1mm every 0.15 turns on the basis of 20mm, and the working length L_0 is 60mm. First, insert the spring-fixing upper circular plate into the reserved gap on the syncretic-bionic corrugated orthogonal layering configuration. The spring-fixing circular plate can not only fix the spring, but also ensure that the syncretic-bionic corrugated orthogonal layering configuration is uniformly compressed during the loading process. Springs corresponding to different equivalent rotation angles ,θ-$_e$. are placed in the grooves of the upper plate and lower cylinder. Thereby adjusting the working length L_0 of the non-uniform spring to achieve the programmable effect of metamaterials.

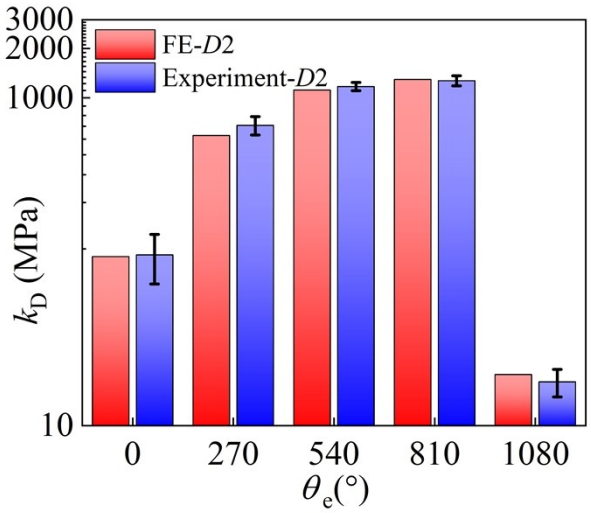

Fig. S10 Relationship between the modulus k_D of Dnon-uniform metamaterial with law D1 and the equivalent rotation angle θ-$_e$.,.

Table S1. Variation of the total working length L_{0T} of the metamaterial based on uniform springs with the rotation angle

$\theta(^\circ)$	$L_{01}(\mathrm{mm})$	$L_{02}(\mathrm{mm})$	$L_{03}(\mathrm{mm})$
0	60	0	60
54	57	3	60
108	54	6	60
162	51	9	60
216	48	12	60
270	45	15	60
324	42	18	60
378	39	21	60
432	36	24	60
486	33	27	60
540	30	30	60
594	27	33	60
648	24	36	60
702	21	39	60
756	18	42	60
810	15	45	60
864	12	48	60
918	9	51	60
972	6	54	60
1026	3	57	60
1080	0	60	60

Define the rotation angle $\theta = 0^\circ$ of an inner spring when it has the longest working length L_{01max}, with clockwise rotation as the positive direction. Define the rotation angle $\theta = 0^\circ$ of another inner spring when it has the shortest working length L_{01min}, with counterclockwise rotation as the positive direction. The height of the metamaterial depends on the greater of the two inner spring working lengths L_{01} and L_{02}.

Table S2. Typical parameter values and variation of the spring compression length for the position angle β of the variable position angle metamaterial group based on uniform springs

$\theta(^\circ)$	$\beta(^\circ)$	$L_{0S}\,(\mathrm{mm})$	$L_{0H}\,(\mathrm{mm})$
0	540	6	46
180	720	4	54
252	792	0	54
360	900	0	54
540	1080	0	54
720	900	0	54
828	792	0	54
900	720	4	54
1080	540	6	46
1260	360	8	38
1440	180	10	30
1620	0	12	22
1800	180	10	30
1980	360	8	38
2160	540	6	46

Table S3. Typical parameter values for the rotation angle θ of the variable rotation angle difference metamaterial group based on uniform springs

$\Delta\theta(^\circ)$	$\theta_1(^\circ)$	$\theta_2(^\circ)$	$\theta_3(^\circ)$	$\theta_4(^\circ)$
0	0	0	0	0
36	0	36	72	108
72	0	72	144	216
108	0	108	216	324
144	0	144	288	432
180	0	180	360	540
216	0	216	432	504
252	0	252	504	288
288	0	288	576	72
324	0	324	504	144
360	0	360	360	360

The working length $L_{0i}(i = 1,2,3,4)$ of lower springs can be calculated based on the values $\theta_i(i = 1,2,3,4)$ in Table S3, and the calculation formula is $L_{0i} = L_0 - t/360^\circ * \theta_i$.

Table S4. Typical parameter values for the position angle β of variable position angle metamaterial group containing four metamaterials

$\theta(^\circ)$	$\beta_1(^\circ)$	$\beta_2(^\circ)$	$\beta_3(^\circ)$	$\beta_4(^\circ)$
0	0	220	440	660
36	36	256	476	696
72	72	292	512	708
108	108	328	548	672
144	144	364	584	636
180	180	400	620	600
216	216	436	656	564
252	252	472	692	528
288	288	508	712	492
324	324	544	676	456
360	360	580	640	420

The working length $L_{0i}(i = 1,2,3,4)$ of lower springs can be calculated based on the values $\beta_i(i = 1,2,3,4)$ in Table S4, and the calculation formula is $L_{0i} = L_0 - t/360^\circ * \beta_i$.

Table S5. Typical parameter values for the position angle β of variable position angle metamaterial group containing five metamaterials

$\theta(^\circ)$	$\beta_1(^\circ)$	$\beta_2(^\circ)$	$\beta_3(^\circ)$	$\beta_4(^\circ)$	$\beta_5(^\circ)$
0	0	220	440	660	560
36	36	256	476	696	524
72	72	292	512	708	488
108	108	328	548	672	452
144	144	364	584	636	416
180	180	400	620	600	380
216	216	436	656	564	344
252	252	472	692	528	308
288	288	508	712	492	272
324	324	544	676	456	236
360	360	580	640	420	200

The working length $L_{0i}(i = 1,2,3,4,5)$ of lower springs can be calculated based on the values $\beta_i(i = 1,2,3,4,5)$ in Table S5, and the calculation formula is $L_{0i} = L_0 - t/360^\circ * \beta_i$.

Table S6. Typical parameter values for the position angle β of variable position angle metamaterial group containing six metamaterials

$\theta(°)$	$\beta_1(°)$	$\beta_2(°)$	$\beta_3(°)$	$\beta_4(°)$	$\beta_5(°)$	$\beta_6(°)$
0	0	220	440	660	560	340
36	36	256	476	696	524	304
72	72	292	512	708	488	268
108	108	328	548	672	452	232
144	144	364	584	636	416	196
180	180	400	620	600	380	160
216	216	436	656	564	344	124
252	252	472	692	528	308	88
288	288	508	712	492	272	52
324	324	544	676	456	236	16
360	360	580	640	420	200	20

The working length $L_{0i}(i = 1,2,3,4,5,6)$ of lower springs can be calculated based on the values $\beta_i(i = 1,2,3,4,5,6)$ in Table S6, and the calculation formula is $L_{0i} = L_0 - t/360° * \beta_i$.

Table S7. Typical parameter values for the position angle β of variable position angle metamaterial group containing seven metamaterials

$\theta(^\circ)$	$\beta_1(^\circ)$	$\beta_2(^\circ)$	$\beta_3(^\circ)$	$\beta_4(^\circ)$	$\beta_5(^\circ)$	$\beta_6(^\circ)$	$\beta_7(^\circ)$
0	0	220	440	660	560	340	120
36	36	256	476	696	524	304	84
72	72	292	512	708	488	268	48
108	108	328	548	672	452	232	12
144	144	364	584	636	416	196	24
180	180	400	620	600	380	160	60
216	216	436	656	564	344	124	96
252	252	472	692	528	308	88	132
288	288	508	712	492	272	52	168
324	324	544	676	456	236	16	204
360	360	580	640	420	200	20	240

The working length $L_{0i}(i = 1,2,3,4,5,6,7)$ of lower springs can be calculated based on the values $\beta_i(i = 1,2,3,4,5,6,7)$ in Table S7, and the calculation formula is $L_{0i} = L_0 - t/360^\circ * \theta_i$.

Table S8. Typical parameter values for the rotation angle θ of the variable rotation angle difference metamaterial group based on Rule 1

$\Delta\theta(^\circ)$	$\theta_1(^\circ)$	$\theta_2(^\circ)$	$\theta_3(^\circ)$	$\theta_4(^\circ)$
0	0	0	0	0
36	0	36	72	108
72	0	72	144	216
108	0	108	216	324
144	0	144	288	72
180	0	180	360	180
216	0	216	72	288
252	0	252	144	36
288	0	288	216	144
324	0	324	288	252
360	0	360	360	360

The working length $L_{0i}(i = 1,2,3,4)$ of lower springs can be calculated based on the values $\theta_i(i = 1,2,3,4)$ in Table S8, and the calculation formula is $L_{0i} = L_0 - t/360^\circ * \theta_i$.

Table S9. Typical parameter values for the rotation angle θ of the variable rotation angle difference metamaterial group based on Rule 2

$\Delta\theta(^\circ)$	$\theta_1(^\circ)$	$\theta_2(^\circ)$	$\theta_3(^\circ)$	$\theta_4(^\circ)$
0	0	0	0	0
36	0	36	72	108
72	0	72	144	216
108	0	108	216	324
144	0	144	288	432
180	0	180	360	600
216	0	216	432	276
252	0	252	708	48
288	0	288	492	372
324	0	324	276	696
360	0	360	60	420

The working length $L_{0i}(i = 1,2,3,4)$ of lower springs can be calculated based on the values $\theta_i(i = 1,2,3,4)$ in Table S9, and the calculation formula is $L_{0i} = L_0 - t/360^\circ * \theta_i$.

Table S10. Pitch *t*, effective number of turns *n* and height information of the pitch non-uniform spring

t (mm)	n	Height (mm)
35	0.06	2.25
34	0.15	5.10
33	0.15	4.95
32	0.15	4.80
31	0.15	4.65
30	0.15	4.50
29	0.15	4.35
28	0.15	4.20
27	0.15	4.05
26	0.15	3.90
25	0.15	3.75
24	0.15	3.60
23	0.15	3.45
22	0.15	3.30
21	0.15	3.15

Table S11. Variation for the maximum compressible length L_a of the pitch non-uniform spring corresponding to the typical equivalent rotation angle θ_e

$\theta_e(^\circ)$	$L_a(\mathrm{mm})$	$\theta_e(^\circ)$	$L_a(\mathrm{mm})$
0	25.37	594	13.56
54	24.66	648	12.17
108	23.84	702	10.76
162	22.94	756	9.31
216	21.97	810	7.82
270	20.93	864	6.32
324	19.83	918	4.77
378	18.68	972	3.21
432	17.46	1026	1.62
486	16.20	1080	0
540	14.90		

Supplementary References

1 T. Claverie, E. Chan and S. N. Patek, *Evolution*, 2011, **65**, 443-461.
2 J. C. Weaver, G. W. Milliron, A. Miserez, K. E. Lutterodt, S. Herrera, I. Gallana, W. L. Mershon, B. Swanson, P. Zavattieri, E. Dimasi and D. Kisailus, *Science*, 2012, **336**, 1275-1280.
3 S. N. Patek, and R. L. Caldwell, *J. Exp. Biol.*, 2005, **208**, 3655-3664.
4 S. N. Patek, W. L. Korff and R. L. Caldwell, *Nature*, 2004, **428**, 819-820.
5 Q. Liu, Z. W. Mo, Y. H. Wu, J. B. Ma, G. C. P. Tsui, and D. Hui, *Compos. B*, 2016, **98**, 409-414.
6 S. A. Lurie, Y. O. Solyaev, A. A. Koshurina, V. F. Formalev, V. N. Dobryanskiy and M. L. Kachanov, *Compos. Struct.*, 2018, **188**, 278-286.
7 K. Liu, S. Zong, Y. Li, Z. P. Wang, Z. Q. Hu and Z. L. Wang, *Mar. Struct.*, 2022, **84**, 103198.
8 D. Chateigner, C. Hedegaard and H. R. Wenk, *J. Struct. Geol.*, 2000, **22**, 1723-1735.
9 D. L. Kaplan, *Solid St. M.*, 1998, **3**, 232-236.
10 B. Vijaya Ramnath, J. Jeykrishnan, G. Ramakrishnan, B. Barath, E. Ejoelavendhan and P. Arun Raghav, *Mater. Today: Proc.*, 2018, **5**, 1846-1851.
11 A. P. Jackson, J. F. V. Vincent, D. Briggs, R. A. Crick, S. F. Davies, M. J. Hearn and R. M. Turner, *J. Mater. Sci. Lett.*, 1986, **5**, 975-978.
12 A. P. Jackson, J. F. V. Vincent and R. M. Turner, *Proc. R. Soc. Lond. B*, 1988, **234**, 415-440.
13 Q. M.Li, I. Magkiriadis and J. J. Harrigan, *J. Cell. Plast.*,2006, **42**, 371-392.